PHYSICAL REVIEW C VOLUME 26, NUMBER 2 AUGUST 1982

Nuclear dynamics and quasi-elastic electron scattering

L. S. Celenza, W. S. Pong, M. M. Rahman,* and C. M. Shakin
Department of Physics and Institute for Nuclear Theory,
Brooklyn College of the City University of New York,
Brooklyn, New York 11210
(Received 10 March 1982)

We present results of calculations of the longitudinal and transverse response function for inelastic electron scattering from ^{56}Fe and ^{12}C. In the impulse approximation it is found that the calculated longitudinal response is approximately forty percent too large for ^{56}Fe. We discuss those aspects of nuclear dynamics which could account for this discrepancy and suggest that the depletion of the shell model orbitals through various (short-range) correlation effects may play an important role. It is suggested that a significant longitudinal response may exist at energies above the quasi-elastic domain; this response would involve the excitation of 2p-2h states. In our model there is a significant disagreement between theory and experiment for the transverse response. We ascribe this disagreement to meson-exchange-current effects; however, we present no calculations of such effects in this work. Quantitative studies of these effects in finite nuclei are required. If our model for the quenching of the longitudinal response in the quasi-elastic domain proves to be correct, we can infer that quasi-elastic electron scattering studies may provide a measurement of the average probability of the occupation of a shell model orbital.

[NUCLEAR REACTIONS Quasi-elastic electron scattering; transverse and longitudinal response functions; finite nucleus calculations in a modified impulse approximation.]

I. INTRODUCTION

One of the most interesting experimental results in recent years has been the separation of the longitudinal and transverse response in inelastic electron scattering for intermediate values of the momentum transfers.[1,2] One striking feature of the analysis has been the failure of the standard Fermi-gas model to explain the data. For example, as may be seen in the figures of Refs. 1 and 3, the Fermi-gas model gives a result that appears satisfactory for the transverse response but is about a factor of 2 too large when the longitudinal response is considered. This discrepancy is particularly difficult to understand since meson-exchange-current corrections are expected to be small for the longitudinal response, although such corrections can be quite important for the transverse response function.[4] Noble has considered this matter and noted that the longitudinal response could be reduced by modifying the nucleon form factor, that is, allowing for a larger proton size in the nuclear medium.[3] In this work we consider an alternative explanation of the nuclear response and argue that the reduction of the longitudinal response may be a more or less direct measure of nuclear correlations which deplete the shell model orbitals. In order to study this question and avoid the uncertainties introduced by the Fermi-gas model we have carried out our calculations using wave functions appropriate to a finite nucleus. The calculations are relativistic in that we solve the Dirac equation to obtain the spinor wave functions of the bound orbitals. The continuum orbitals are solutions of the free Dirac equation. The details of the calculation are presented in the following section. However, it is useful to summarize our results at this point.

Our calculations do not contain any free parameters and we find that for both ^{56}Fe and ^{12}C we obtain a good agreement with the shape and peak position of the experimental curve in the quasi-elastic region. Without any modifications, the calculated

transverse response is in fair agreement with the data while the longitudinal response is uniformly too large. If we multiply our cross sections for ^{56}Fe by 0.6 and those for ^{12}C by about 0.7 the longitudinal response is given correctly. This procedure now leads to more marked disagreement between the calculated and measured transverse response. We believe that the effects of meson-exchange currents which enhance the transverse response may account for this discrepancy. We further assume that it is important to construct a model which fits the longitudinal response, since corrections from meson currents are small in this case.[4,5]

We should also note that final-state interaction effects in inclusive electron scattering have also been studied.[6] The effects are not particularly large and lead to a reduction of the peak height by 5 to 10 percent. We refer the reader to Ref. 6 for a discussion of this effect.

In the following sections we present arguments to indicate that the factors 0.6 and 0.7 mentioned above can be interpreted as the square of a wave function renormalization constant. That is, in the case of ^{56}Fe we expect an occupation probability of $\sqrt{0.6}\simeq 0.8$ for each orbital.[7] (For ^{12}C the corresponding probability is somewhat larger since ^{12}C is a less dense system.) Essential to our argument is the observation that the depletion of the shell-model orbitals mentioned above is due to the short-range ("hard-core") and tensor parts of the nucleon-nucleon interaction. Thus each particle orbital has admixed 2p-1h states in which the particle states have large momenta. As we will discuss later in the work, this has the effect of shifting strength out of the quasi-elastic peak to higher energies. If our interpretation of the data is correct we can conclude that quasi-elastic electron scattering may be used to obtain a fairly direct measure of the depletion of nucleon orbitals due to short-range correlations. Of course, to obtain a truly quantitative measure of orbital occupation probabilities it will be necessary to have good theoretical estimates for the effects of meson-exchange currents.

The plan of our work is as follows. In Sec. II we review some aspects of the theory of quasi-elastic electron scattering and present the results of our calculations. In Sec. III we discuss those aspects of many-body theory that are useful for the considerations of this work and we indicate how we may improve upon the impulse approximation. We also discuss how considerations of unitarity aid in understanding the dynamics. In Sec. IV we discuss the experimental data for ^{56}Fe and ^{12}C. Finally, in Sec. V we present some concluding remarks.

II. QUASI-ELASTIC ELECTRON SCATTERING

The electron scattering cross section is usually written as (see Fig. 1)

$$\frac{d^2\sigma}{d\Omega_2 dE_2}=\frac{Z^2}{M_T}\sigma_M[\,W_2(|\vec{q}|,\omega) -2W_1(|\vec{q}|,\omega)\tan^2\tfrac{1}{2}\theta]\,, \tag{2.1}$$

where the Mott differential cross section σ_M is given by

$$\sigma_M=\frac{\alpha^2}{4E_1^{\,2}}\frac{\cos^2(\theta/2)}{\sin^4(\theta/2)}\,. \tag{2.2}$$

Here M_T is the mass of the target. The longitudinal and transverse response functions are given by

$$S_L(|\vec{q}|,\omega)=\frac{Z^2}{4\pi}\frac{|\vec{q}|^2}{q^2}[-W_1(|\vec{q}|,\omega) +\frac{|\vec{q}|^2}{q^2}W_2(|\vec{q}|,\omega)] \equiv(M_T/4\pi)R_L(|\vec{q}|,\omega) \tag{2.3}$$

and

$$S_T(|\vec{q}|,\omega)=(Z^2/4\pi)[-2W_1(|\vec{q}|,\omega)] \equiv(M_T/4\pi)R_T(|\vec{q}|,\omega)\,. \tag{2.4}$$

We shall be using the Bjorken and Drell convention so that $q^2=\omega^2-|\vec{q}|^2$.

The functions W_1 and W_2 appear in the response tensor $\mathscr{W}_{\mu\nu}$ which may be written in the laboratory frame as

$$\mathscr{W}^{\mu\nu}=W_1 g^{\mu\nu}+\hat{P}^\mu\hat{P}^\nu W_2 =(2\pi)^6\frac{M_T}{Z^2}\sum_{P_x}\langle P_x|J_\nu^N(0)|P\rangle^* \times\langle P_x|J_\mu^N(0)|P\rangle \times\delta^4(P+q-P_x)\,. \tag{2.5}$$

Here

$$\hat{P}^\mu=(P^\mu-(q\cdot P)q^\mu/q^2)/M_T\,.$$

The quantity in the square brackets in Eq. (2.1) is $\hat{N}_e^{\mu\nu}\mathscr{W}_{\mu\nu}$, where

$$\hat{N}_e^{\mu\nu}=\tfrac{1}{2}\mathrm{Tr}[\gamma^\mu(\not k_1+m_e)\gamma^\nu(\not k_2+m_e)]/[4E_1E_2\cos^2(\theta/2)]$$
$$=[k_1^\mu k_2^\nu+k_2^\mu k_1^\nu+g^{\mu\nu}(q^2/2)]/[2E_1E_2\cos^2(\theta/2)]\ . \tag{2.6}$$

For the matrix elements of the nuclear current in Eq. (2.5) we have taken (see Fig. 1),

$$\langle \vec{p}_N,s;-\vec{Q}JLM \mid J_\mu^N(0)\mid \vec{P}\rangle=\langle \vec{p}_N,s\mid\bar{\psi}(0)\mid 0\rangle\Gamma_\mu(q)\langle -\vec{Q}JLM\mid\psi(0)\mid P\rangle\ . \tag{2.7}$$

Here

$$\Gamma_\mu(q)=\gamma_\mu F_1(q^2)+i\sigma^{\mu\nu}q_\nu\left[\frac{\kappa}{2M_N}\right]F_2(q^2)\ , \tag{2.8}$$

with $F_1^P(0)=F_2^P(0)=1$; $F_1^n(0)=0$, $F_2^n(0)=1$; $\kappa_P=1.793$, $\kappa_n=-1.913$. Also,

$$\langle \vec{p}_N,s\mid\bar{\psi}(0)\mid 0\rangle=\left[\frac{M_N}{E_N(\vec{p}_N)}\right]^{1/2}\bar{u}_s(\vec{p}_N)(2\pi)^{-3/2} \tag{2.9}$$

and

$$\langle -\vec{Q}JLM\mid\psi(0)\mid P\rangle=(2\pi)^{-3/2}\psi_{JLM}(\vec{Q})\ . \tag{2.10}$$

The bound-state wave functions $\psi_{JLM}(\vec{Q})$ are the Fourier transforms of the solutions of the Dirac radial equation:

$$\left\{\frac{1}{i}\vec{\alpha}\cdot\vec{\nabla}+\beta[M_N+S(r)]+V(r)\right\}\psi_{JLM}(\vec{r})=(M_N-\epsilon_{JL})\psi_{JLM}(\vec{r})\ . \tag{2.11}$$

Here $S(r)$ and $V(r)$ are scalar and vector potentials corresponding to a self-energy

$$\Sigma(r)=S(r)+\beta V(r)\ .$$

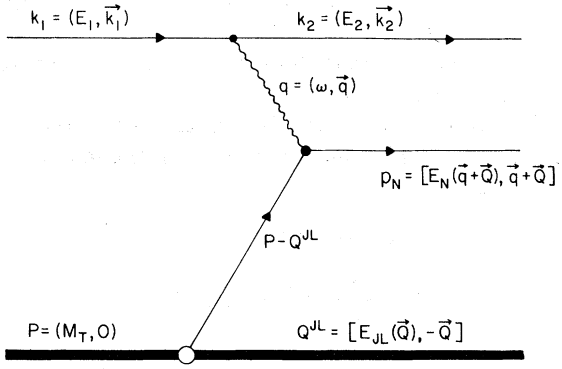

FIG. 1. Basic diagram used to calculate the quasielastic process. Here

$$E_{JL}(\vec{Q})=[M_{JL}{}^2+\vec{Q}^2]^{1/2}$$

and

$$E_N(\vec{q}+\vec{Q})=[M_N{}^2+(\vec{q}+\vec{Q})^2]^{1/2}$$

with M_{JL} and M_N the mass of the residual nucleus and the nucleon, respectively. The heavy solid line denotes the nuclear target or the residual nucleus and the wavy line is a virtual photon.

As usual we put

$$\psi_{JLM}(\vec{r})=\frac{1}{r}\begin{bmatrix}F_{JL}(r)\mathscr{Y}_L^{JM}(\hat{r})\\ iG_{JL'}(r)\mathscr{Y}_{L'}^{JM}(\hat{r})\end{bmatrix}\ , \tag{2.12}$$

and write

$$\psi_{JLM}(\vec{Q})=i^L\int\frac{e^{-i\vec{Q}\cdot\vec{r}}}{(2\pi)^{3/2}}\psi_{JLM}(\vec{r})d\vec{r}$$
$$=\begin{bmatrix}R_u^{JL}(Q)\mathscr{Y}_L^{JM}(\hat{Q})\\ R_l^{JL}(Q)(\vec{\sigma}\cdot\hat{Q})\mathscr{Y}_L^{JM}(\hat{Q})\end{bmatrix}\ , \tag{2.13}$$

where

$$R_u^{JL}(Q)=\int_0^\infty F^{JL}(r)j_L(Qr)r\,dr\sqrt{2/\pi}\ , \tag{2.14}$$

$$R_l^{JL}(Q)=(-1)^{(L'-L+1)/2}\times\int_0^\infty G^{JL'}(r)j_{L'}(r)r\,dr\sqrt{2/\pi}\ . \tag{2.15}$$

If we insert Eqs. (2.7)–(2.10) into Eq. (2.5) we find

$$\mathscr{W}^{\mu\nu}=\sum_{JL}\mathscr{W}_{JL}^{\mu\nu}\ , \tag{2.16}$$

where

$$\mathscr{W}^{\mu\nu}_{JL}=\frac{M_T}{Z^2}\int d\vec{Q}\left[\frac{M_N}{E_N(\vec{p}_N)}\right]\times\delta(\omega+M_T-E_{JL}(\vec{Q})-E_N(\vec{p}_N))\times T^{\mu\nu}_{JL}(2M_N)^{-1}\,, \tag{2.17}$$

$$T^{\mu\nu}_{JL}=\mathrm{Tr}\left\{\left[\gamma^\nu F_1-i\sigma^{\nu\rho}q_\rho\left[\frac{\kappa}{2M_N}\right]F_2\right]\times(\not{p}_N+M_N)\times\left[\gamma^\mu F_1+i\sigma^{\mu\lambda}q_\lambda\left[\frac{\kappa}{2M_N}\right]F_2\right]\rho_{JL}(Q)\right\}. \tag{2.18}$$

Here the target density matrix $\rho_{JL}(Q)$ is given by

$$\rho_{JL}(Q)=\sum_M\psi_{JLM}(\vec{Q})\bar{\psi}_{JLM}(\vec{Q})=A_{JL}(Q)+\not{B}_{JL}(Q)\,, \tag{2.19}$$

where

$$A_{JL}(Q)=\left[\frac{2J+1}{8\pi}\right][(R^{JL}_u(Q))^2-(R^{JL}_l(Q))^2]/2\,, \tag{2.20}$$

$$B^0_{JL}(Q)=\left[\frac{2J+1}{8\pi}\right][(R^{JL}_u(Q))^2+(R^{JL}_l(Q))^2]/2\,, \tag{2.21}$$

$$\vec{B}_{JL}(Q)=\left[\frac{2J+1}{8\pi}\right]\hat{Q}R^{JL}_u(Q)R^{JL}_l(Q)\,. \tag{2.22}$$

The trace $T^{\mu\nu}_{JL}$ is given by

$$T^{\mu\nu}_{JL}=4M_N\left\{\left[A_{JL}\left[F_1{}^2+F_2{}^2\left[\frac{\kappa}{2M_N}\right]^2q^2\right]+2\left[\frac{\kappa}{2M_N}\right]F_1F_2q\cdot\left[A_{JL}\frac{p_N}{M_N}-B_{JL}\right]\right.\right.$$
$$-[F_1{}^2-F_2{}^2(\kappa/2M_N)^2q^2](p_N\cdot B_{JL})/M_N-2F_2{}^2\left[\frac{\kappa}{2M_N}\right]^2(p_N\cdot q)(B_{JL}\cdot q)/M_N\Big]g^{\mu\nu}$$
$$\left.+\left[F_1{}^2-F_2{}^2\left[\frac{\kappa}{2M_N}\right]^2q^2\right]\left[\frac{p^\mu_N}{M_N}B^\nu_{JL}+B^\mu_{JL}\frac{p^\nu_N}{M_N}\right]\right\}. \tag{2.23}$$

Note that if we replace B^μ_{JL} by p^μ_i and A_{JL} by M_N we find the free-nucleon trace

$$T^{\mu\nu}\to 4M_N\left\{\frac{q^2}{2M_N}[F_1+\kappa F_2]^2g^{\mu\nu}+2\left[F_1{}^2-F_2{}^2\left[\frac{\kappa}{2M_N}\right]^2q^2\right]\frac{p^\mu_ip^\nu_i}{M_N}\right\}. \tag{2.24}$$

In addition, for the purposes of the following discussion, we write

$$T^{\mu\nu}_{JL}=4\{g^{\mu\nu}T_1+(p^\mu_NB^\nu_{JL}+p^\nu_NB^\mu_{JL})T_2\}\,, \tag{2.25}$$

where $T_{1,2}$ are given by comparison with Eq. (2.23). Since $T^{\mu\nu}_{JL}$ is not gauge invariant we define

$$\hat{T}^{\mu\nu}_{JL}=\left[g^{\mu\lambda}-\frac{q^\mu q^\lambda}{q^2}\right]T^{\lambda\gamma}_{JL}\left[g^{\gamma\nu}-\frac{q^\gamma q^\nu}{q^2}\right]$$
$$=4\left[\left[g^{\mu\nu}-\frac{q^\mu q^\nu}{q^2}\right]T_1+(p^\mu_N\hat{B}^\nu_{JL}+\hat{p}^\nu_N\hat{B}^\mu_{JL})T_2\right], \tag{2.26}$$

where

$$\hat{p}_N^{\mu}=p_N^{\mu}-(p_N\cdot q)q^{\mu}/q^2 ,$$

etc. Further we form the kernels appropriate to the calculation of W_1^{JL}, W_2^{JL} [see Eq. (2.5)]:

$$w_1^{JL}=T_1+T_2\left\{\hat{p}_N\cdot\hat{B}_{JL}-\frac{(\hat{p}_N\cdot P)(\hat{B}_{JL}\cdot P)/M_T{}^2}{[1-(P\cdot q)^2/(q^2M_T{}^2)]}\right\}, \tag{2.27}$$

$$w_2^{JL}=T_2\left[3(\hat{p}_N\cdot P)(\hat{B}_{JL}\cdot P)/M_T{}^2-\hat{p}_N\cdot\hat{B}_{JL}\left[1-\frac{(q\cdot P)^2}{q^2M_T{}^2}\right]\right][1-(q\cdot P)^2/(q^2M_T{}^2)]^{-2} . \tag{2.28}$$

In terms of $w_{1,2}^{JL}$ we have

$$W_{1,2}^{JL}=\frac{M_T}{Z^2}\int\frac{d\vec{Q}}{2E_N(\vec{p}_N)}\delta(\omega+M_T-E_{JL}(\vec{Q})-E_N(\vec{p}_N))w_{1,2}^{JL} . \tag{2.29}$$

Since w_i^{JL} depends only upon $\cos(\hat{q}\cdot\hat{Q})$, we may reduce the integrals required in the calculation of W_1^{JL} and W_2^{JL} to

$$W_i^{JL}=\frac{\pi}{|\vec{q}|}\frac{M_T}{Z^2}\int_{Q_l}^{Q_u}w_i^{JL}(|\vec{q}|,\omega,|\vec{Q}|,\cos\theta^*)Q\,dQ . \tag{2.30}$$

Here

$$\cos\theta^*(|\vec{q}|,|\vec{Q}|,\omega)=\{[\omega+M_T-E_{JL}(\vec{Q})]^2-[M_N{}^2+|\vec{Q}|^2+|\vec{q}|^2]\}/(2|\vec{Q}||\vec{q}|) ,$$

where

$$E_{JL}(\vec{Q})=[|\vec{Q}|^2+M_{JL}{}^2]^{1/2}$$

with (2.31)

$$M_{JL}=M_T-M_N+\epsilon_{JL} .$$

Further

$$Q_u=a+b , \tag{2.32}$$

$$Q_l=|a-b| , \tag{2.33}$$

with

$$a=\frac{\omega+M_T}{2}\left[\left\{1-\frac{(M_{JL}+M_N)^2}{\Lambda^2}\right\}\times\left\{1-\frac{(M_{JL}-M_N)^2}{\Lambda^2}\right\}\right]^{1/2} , \tag{2.34}$$

$$b=\frac{|\vec{q}|}{2}\left\{1+\frac{M_{JL}{}^2-M_N{}^2}{\Lambda^2}\right\} , \tag{2.35}$$

and

$$\Lambda^2=(\omega+M_T)^2-|\vec{q}|^2 . \tag{2.36}$$

In the nonrelativistic limit

$$\cos\theta^*\rightarrow\left\{\omega-\epsilon_{JL}-\frac{(|\vec{Q}|^2+|\vec{q}|^2)}{2M_N}\right\}\times\left\{\frac{M_N}{|\vec{q}||\vec{Q}|}\right\} , \tag{2.37}$$

$$a\rightarrow[2(\omega-\epsilon_{JL})M_N]^{1/2} , \tag{2.38}$$

$$b\rightarrow|\vec{q}| . \tag{2.39}$$

Results of our calculations for the transverse and longitudinal response functions, S_T and S_L, are shown in Figs. 2 and 3. We will call the response shown in Figs. 2 and 3 the unmodified impulse approximation result. These results may be compared with the experimental data given in Ref. 1. In the next section we will make such a comparision. ever, before proceeding we will discuss the theoretical basis for introducing a *modified* impulse approximation.

III. SOME ASPECTS OF MANY-BODY THEORY

In the Introduction we noted that a direct application of the impulse approximation failed to ex-

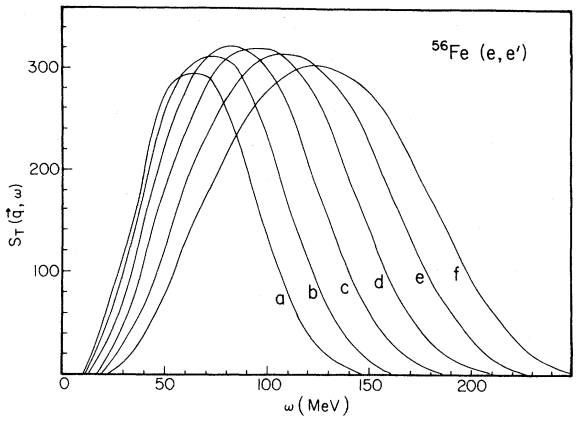

FIG. 2. Unmodified impulse approximation results for the transverse response function, $S_T(\vec{q},\omega)$, as a function of energy transfer for ^{56}Fe and for various values of $|\vec{q}|$: (a) $q=210$ MeV/c, (b) $q=250$ MeV/c, (c) $q=290$ MeV/c, (d) $q=330$ MeV/c, (e) $q=370$ MeV/c, and (f) $q=410$ MeV/c.

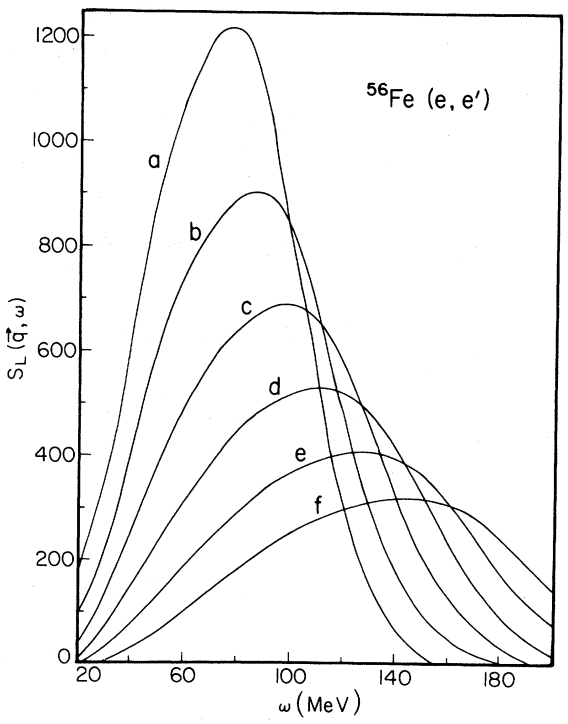

FIG. 3. Unmodified impulse approximation results for the longitudinal response function, $S_L(\vec{q},\omega)$, as a function of energy transfer for various values of $|\vec{q}|$: (a) $q=210$ MeV/c, (b) $q=250$ MeV/c, (c) $q=290$ MeV/c, (d) $q=330$ MeV/c, (e) $q=370$ MeV/c, and (f) $q=410$ MeV/c.

plain the longitudinal response function for quasi-elastic electron scattering. (The disagreement with the data for the transverse response function was not as large.) In this section we will discuss a modified impulse approximation. For simplicity we will first consider the photon polarization operator in nuclear matter and then use this discussion to provide a basis for modifying our theoretical results.

It is well known that the differential cross section for electron scattering in a uniform medium is given by[8]

$$\frac{1}{\sigma_M}\frac{d^2\sigma}{d\Omega\, dE}=-\frac{V}{\pi}\mathrm{Im}\Pi(\vec{q},\omega)\,, \tag{3.1}$$

where σ_M is the Mott cross section, V is the volume of the target (considered to be a uniform system), and $\Pi(\vec{q},\omega)$ is the polarization operator. Here we are limiting our considerations to the longitudinal response. If one puts

$$\frac{Z}{V}=\rho_0=k_F{}^3/3\pi^2\,, \tag{3.2}$$

where ρ_0 is the density of charged scatterers, one has[8]

$$\frac{1}{\sigma_M}\frac{d^2\sigma}{d\Omega\, dE}=-\frac{3\pi Z}{k_F{}^3}\mathrm{Im}\Pi(\vec{q},\omega)\,. \tag{3.3}$$

The impulse approximation corresponds to the simplest approximation to $\Pi(\vec{q},\omega)$ which is shown in Fig. 4. In this case

$$\Pi_0(\vec{q},\omega)=\frac{-2i}{\hbar}\frac{1}{(2\pi)^4}\int d^4k\, G^0(k)G^0(k+q) \tag{3.4}$$

$$=\frac{2}{(2\pi)^3\hbar}\int d^3k\left[\frac{\theta(|\vec{q}+\vec{k}|-k_F)\theta(k_F-|\vec{k}|)}{\omega+\omega_{\vec{k}}-\omega_{\vec{k}+\vec{q}}+i\eta}-\frac{\theta(k_F-|\vec{q}+\vec{k}|)\theta(|\vec{k}|-k_F)}{\omega+\omega_{\vec{k}}-\omega_{\vec{q}-\vec{k}}-i\eta}\right]. \tag{3.5}$$

where $\omega_{\vec{k}}=k^2/2m$, etc. In evaluating Eq. (3.4) one uses

$$G^0_{\alpha\beta}(\vec{k},\omega)=\delta_{\alpha\beta}\left[\frac{\theta(|\vec{k}|-k_F)}{\omega-\omega_{\vec{k}}+i\eta}+\frac{\theta(k_F-|\vec{k}|)}{\omega-\omega_{\vec{k}}-i\eta}\right], \tag{3.6}$$

where α and β are spin-isospin indices. [The factor of 2 in Eq. (3.5) arises from a spin summation.] Explicit expressions for the polarization operator in this approximation are given in Ref. 8. (In realistic calculations one must include the nucleon electromagnetic form factors.)

As may be seen from inspection of Fig. 1 of Ref. 1, an attempt to fit the response function using this form of the impulse approximation in the context of the Fermi-gas model has similar defects as the unmodified impulse approximation described in the last section. In particular, the calculated longitudinal response is too large.

In order to go beyond the impulse approximation we consider the approximation to the polarization operator in which we use self-consistent Green's functions in Eq. (3.4). That is, instead of $G^0_{\alpha\beta}$ of Eq. (3.6), we use the Green's function of an interacting system. This function may be written as the sum of two terms, one of which has a right hand cut and one of which has a left hand cut in the complex ω plane:

$$G_{\alpha\beta}(\vec{k},\omega)=\delta_{\alpha\beta}\left[\frac{\theta(|\vec{k}|-k_F)}{\omega-\omega_{\vec{k}}-\Sigma(\vec{k},\omega+i\eta)+i\eta}+\frac{\theta(k_F-|\vec{k}|)}{\omega-\omega_{\vec{k}}-\Sigma(\vec{k},\omega-i\eta)-i\eta}\right] . \tag{3.7}$$

Here $\Sigma(\vec{k},\omega)/\hbar$ is the nucleon self-energy. One usually writes, for $\omega\simeq\omega_{\vec{k}}$ and $\Sigma(\vec{k},\omega)=\Sigma_R(\vec{k},\omega)+i\Sigma_{Im}\times(\vec{k},\omega)$,

$$\Sigma_R(\vec{k},\omega)=\Sigma_R(\vec{k},\omega_{\vec{k}})+(\omega-\omega_{\vec{k}})\frac{\partial\Sigma_R}{\partial\omega}(\vec{k},\omega)\,|_{\omega=\omega_{\vec{k}}}+\cdots ,$$

to obtain

$$G_{\alpha\beta}(\vec{k},\omega)\simeq\delta_{\alpha\beta}\left[\frac{Z(\vec{k})\theta(|\vec{k}|-k_F)}{\omega-\omega_{\vec{k}}-\Sigma'(\vec{k},\omega_{\vec{k}}+i\eta)+i\eta}+\frac{Z(\vec{k})\theta(k_F-|\vec{k}|)}{\omega-\omega_{\vec{k}}-\Sigma'(\vec{k},\omega_{\vec{k}}-i\eta)-i\eta}\right] , \tag{3.8}$$

where

$$Z(\vec{k})=\left[1-\frac{\partial\Sigma_R}{\partial\omega}(\vec{k},\omega)\bigg|_{\omega=\omega_{\vec{k}}}\right]^{-1} \tag{3.9}$$

is the wave function renormalization constant and

$$\Sigma'(\vec{k},\omega_{\vec{k}})=Z(\vec{k})\Sigma(\vec{k},\omega_{\vec{k}}) .$$

Note that the expression given in Eq. (3.8) is accurate near the quasi-particle pole at

$$\omega\simeq\omega_{\vec{k}}+\Sigma'(\vec{k},\omega_{\vec{k}}) .$$

In addition to the quasi-particle pole, $G(\vec{k},\omega)$ of Eq. (3.7) has a cut structure associated with the analytic properties of $\Sigma(\vec{k},\omega)$. If we use the model for $\Sigma(\vec{k},\omega)$ shown in Fig. 5(a) we see that this cut structure involves the coupling of the quasi-particle to 2p-1h states.

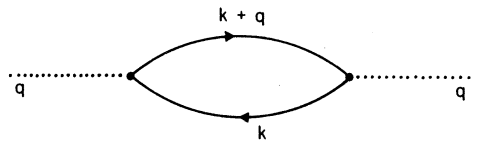

FIG. 4. Basic diagram for the calculation of the polarization operator, $\Pi_0(\vec{q},\omega)$. An integration over k is implied. [See Eqs. (3.4) and (3.5).] The dotted line denotes a photon of four momentum $q=(\vec{q},\omega)$. The crossed diagram is not shown.

The equation for $G(\vec{k},\omega)$,

$$G(\vec{k},\omega)=G^0(\vec{k},\omega)+G^0(\vec{k},\omega)\Sigma(\vec{k},\omega)G(\vec{k},\omega) , \tag{3.10}$$

is shown in Fig. 5(b), where a heavy line is used to denote $G(\vec{k},\omega)$ and a light line is used for $G^0(\vec{k},\omega)$. The perturbation expansion for $\Sigma(\vec{k},\omega)$ indicated in Fig. 5(a) may be used to provide a corresponding expansion for $G(\vec{k},\omega)$, as in Fig. 5(b). In this figure we have indicated the renormalization of the pole term by the factor Z. [There is also a shift in the position of the pole as may be seen upon inspection of Eq. (3.8).] If we neglect the low-lying collective modes, which become relatively less important with increasing momentum transfer, the intermediate particle states appearing in $\Sigma(\vec{k},\omega)$ or $G(\vec{k},\omega)$ have quite high momenta as these excitations are induced by the strong short-range parts of the nucleon-nucleon interaction.

At this point we may exhibit in Fig. 6 a diagrammatic representation of the polarization operator appropriate for the calculation of the longitudinal response. Here the heavy lines denote the Green's functions of Eq. (3.8) and the dark triangle is a vertex function. If we use the equation for the vertex

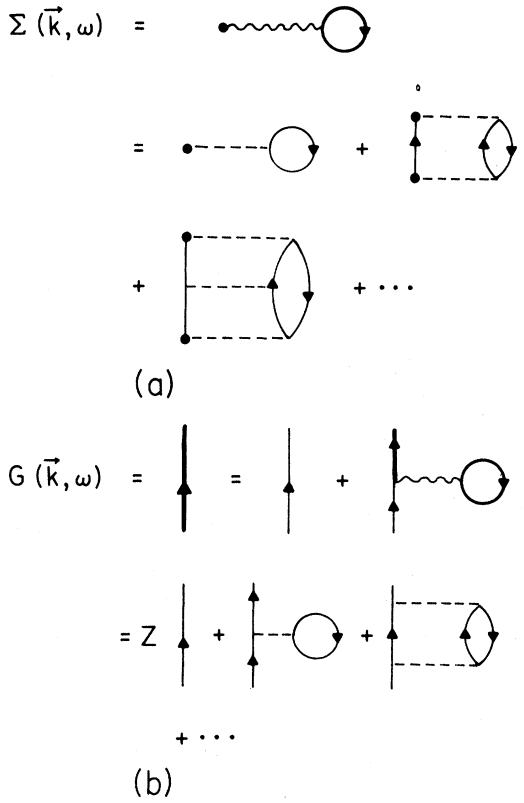

FIG. 5. (a) The self-energy of a nucleon. Here the wavy line denotes a T matrix and the dashed line is a potential interaction. (Only the direct terms are shown.) In this figure we limit ourselves to the term of the self-energy containing a single T matrix. (b) Diagrammatic representation of the equation for $G(\vec{k},\omega)$. The heavy line represents $G(\vec{k},\omega)$ and the light line is $G^0(\vec{k},\omega)$. The wavy line is a T matrix and the dashed lines are potential interactions. (Only the direct terms are shown for simplicity.)

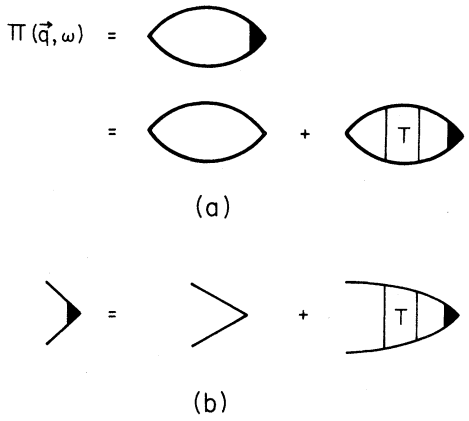

FIG. 6. Diagrammatic representation of the integral equations appropriate to the calculation of the longitudinal part of the polarization operator. (a) Here the heavy lines denote the Green's function of Eq. (3.7). The dark triangle is a vertex function. (b) Schematic representation of the integral equation determining the vertex function. Here T is a nucleon-nucleon scattering amplitude. Use of this equation leads to the second line of part (a) of the figure.

function shown in Fig. 6(b) we obtain the second line of Fig. 6(a). Here T denotes a particle-hole scattering amplitude. Further analysis of this equation for the polarization operator could lead to a description of the response in the random phase approximation (RPA), for example. Calculations which will be reported elsewhere indicate that collective effects are not completely negligible in the longitudinal response at intermediate values of the momentum transfer; however, in a first approximation we can drop the term describing particle-hole rescattering. (We will comment at a later point concerning the uncertainties in the model which are introduced by the neglect of collective aspects of the nuclear response.)

Thus we are motivated to consider a calculation of $\mathrm{Im}\Pi(\vec{q},\omega)$ which involves only the Green's functions of Eq. (3.7). Further, let us also restrict ourselves for the moment to the use of only the pole terms of $G(\vec{k},\omega)$ given in Eq. (3.8). (See Fig. 7.) Except for some effects associated with the detailed structure of $\Sigma'(\vec{k},\omega_{\vec{k}})$, we see that, if $Z(\vec{k})$ is not strongly dependent on k, the result is

$$\Pi(\vec{q},\omega)\simeq Z^2\Pi_0(\vec{q},\omega)\ . \tag{3.11}$$

We suggest that Eq. (3.11) is a useful approximation if $|\vec{q}|$ is large and $\mathrm{Im}\Pi_0(\vec{q},\omega)\neq 0$, that is, in the quasi-elastic scattering region. The basis of this argument may be illustrated as in Fig. 7. The first part of this figure shows $\Pi(\vec{q},\omega)$ expressed in terms of the Green's functions $G(\vec{k},\omega)$ of Eqs. (3.7) and (3.10). These Green's functions may be expanded as in Fig. 5(b) and two terms arising from such an expansion are shown in Fig. 7. The first of these terms corresponds to $Z^2\Pi_0(\vec{q},\omega)$. The second of these terms shows the coupling of the photon to 2p-2h states *via* the strong interaction. The last diagram shows the photon interacting with a highly excited nucleon ($k \gg k_F$) already present in the correlated target. In order to generate this term one must go beyond the model for the self-energy shown in Fig. 5 and include terms quadratic in the T matrix (rearrangement terms).

Now, if the momentum transfer in the strong interaction, $\vec{q}'$, is large, the intermediate 2p-2h states can have large energies placing them above the

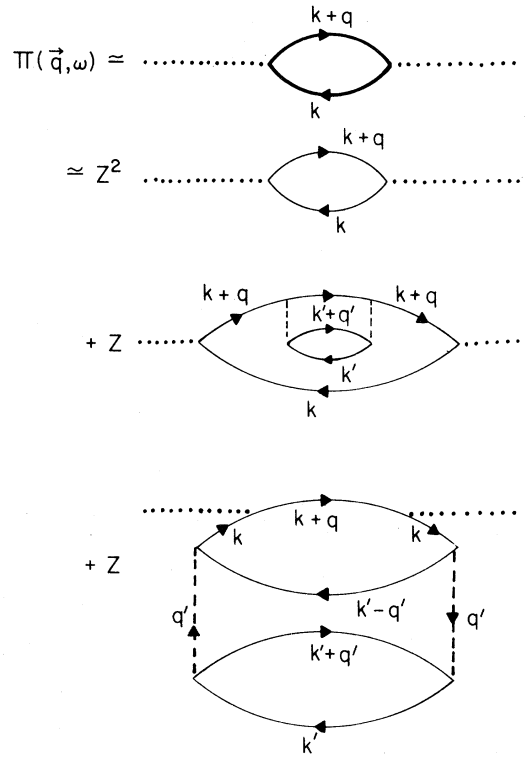

FIG. 7. The photon polarization tensor $\Pi(\vec{q},\omega)$ in the approximation considered in this work. The heavy lines are Green's functions $G(k)$ and $G(k+q)$ while the light lines are $G^0(k)$, . . . , etc. The dashed lines denote potential interactions. [See Fig. 5(b).] Here Z denotes the wave function renormalization constant. Note that the second diagrammatic expansion for $\Pi(\vec{q},\omega)$ is written in terms of Goldstone diagrams. Crossed diagrams are not shown. To obtain the last diagram shown one must consider terms of the self-energy of higher order in the T matrix than those shown in Fig. 5.

quasi-elastic region. Thus the reduction of $\mathrm{Im}\Pi(\vec{q},\omega)$ in the quasi-elastic domain (by the factor Z^2) is compensated by finite values of $\mathrm{Im}\Pi(\vec{q},\omega)$ for energies above the quasi-elastic region. We may now explore the consequences of our assumptions.

IV. COMPARISON OF THE EXPERIMENTAL DATA AND THE MODIFIED IMPULSE APPROXIMATION

In the last section we presented an argument indicating that short-range correlation effects lead to a renormalization of the impulse approximation result by a factor Z^2 in the quasi-elastic domain and an associated enhancement of the response at higher

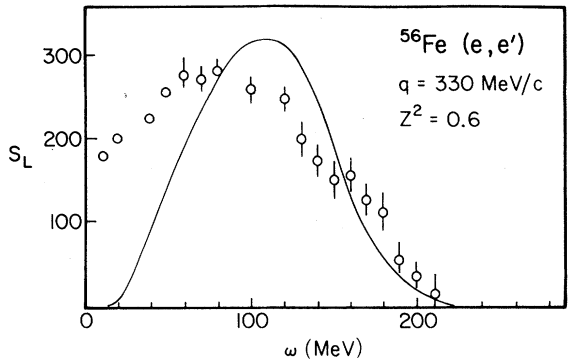

FIG. 8. The modified impulse approximation ($Z^2=0.6$) for $S_L(\vec{q},\omega)$ for ^{56}Fe. Here $|\vec{q}|=330$ MeV/c. The data are from Ref. 1.

energies. We now note that calculations of occupation factors in finite nuclei give $0.77 \leq Z \leq 0.84$. The range of values is associated with different assumptions concerning the intermediate state spectrum in a reaction matrix calculation in the finite system.[7] The occupation factor is more or less independent of the orbital and for definiteness will take $Z^2=0.6$. It is clear from Eq. (3.11) that the inclusion of this factor will lower the theoretical value for the longitudinal response by about 36 percent. In Figs. 8—10 we compare the data for the longitudinal response for ^{56}Fe with the theoretical curves where the impulse approximation result has been reduced by a factor of 0.6. In general, the agreement of the modified curves with the data is satisfactory. The situation with respect to the transverse response is now more complicated. Upon inspection of Figs. 11—13 we see that the disagreement between the

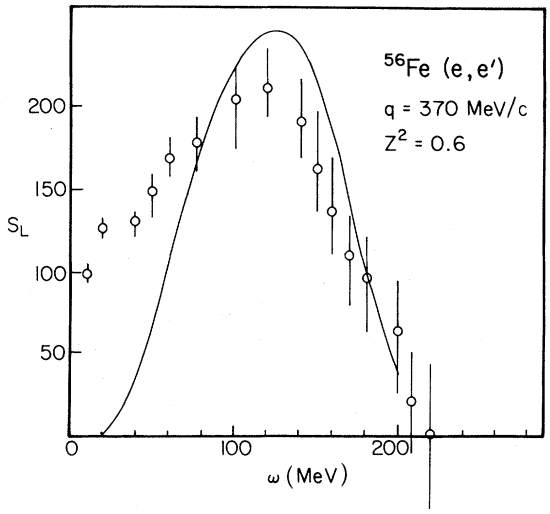

FIG. 9. Same as Fig. 8, except that $|\vec{q}|=370$ MeV/c.

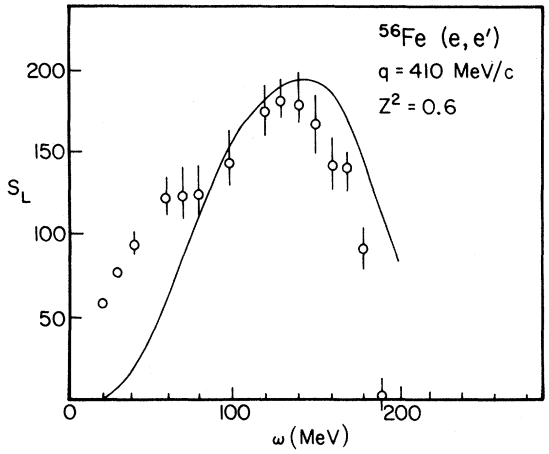

FIG. 10. Same as Fig. 8, except that $|\vec{q}|=410$ MeV/c.

theoretical curves (which represent 0.6 times the unmodified impulse approximation) becomes more marked as we go from $q=210$ MeV/c to $q=410$ MeV/c. It is worth noting that the *unmodified* theoretical result at $q=210$ MeV/c is about 20 percent higher than the data at the peak, while the modified result is about 30 percent too low at the peak. (See Fig. 11.) At $q=250$ MeV/c the modified result is about 40 percent too low while the unmodified result is about 10 percent too large at the peak. (See Fig. 12.)

Upon inspection of the figures for the transverse response function it would appear that the unexplained discrepancy is dependent upon the momentum transfer $|\vec{q}|$. Comparison of the modified impulse approximation with the experimental data indicates that the discrepancy at the peak of the cross section varies *roughly* as $\vec{q}^2$ as one goes from $|\vec{q}|=210$ MeV/c to 410 MeV/c. This suggests that the discrepancy may have its origin in some effect due to meson-exchange currents.

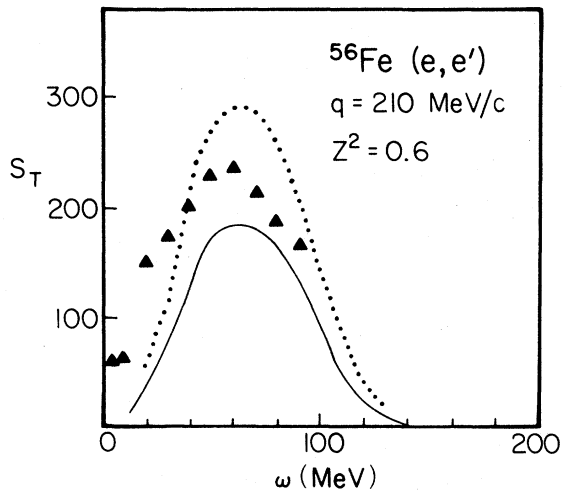

FIG. 11. The unmodified and modified impulse approximation for $S_T(\vec{q},\omega)$ for ^{56}Fe. Here $|\vec{q}|=210$ MeV/c. The data are from Ref. 1. The dotted line is the unmodified response. [See Fig. 2 for the unmodified response at other values of $|\vec{q}|$.]

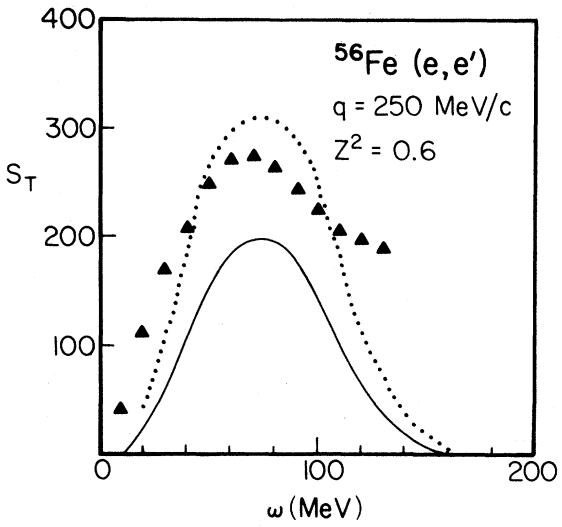

FIG. 12. Same as Fig. 11, except that $|\vec{q}|=250$ MeV/c.

In the previous section we remarked that some uncertainty was introduced into the analysis due to the possibility of some collective effects in the longitudinal response. An indication of this feature is seen upon further inspection of Figs. 8—10 and Fig. 14. In these figures we note a significant amount of

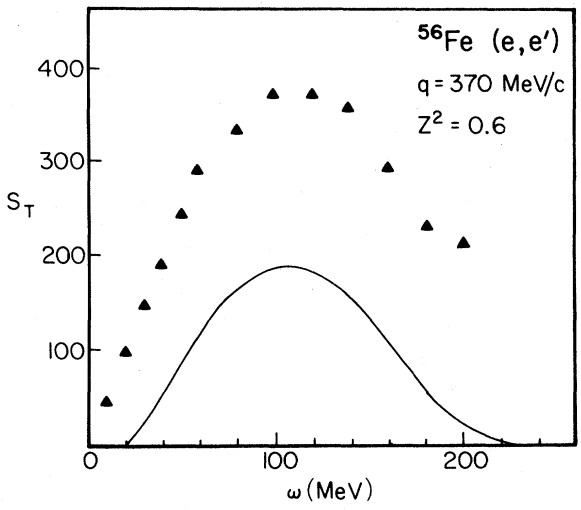

FIG. 13. Same as Fig. 11, except that $|\vec{q}|=370$ MeV/c.

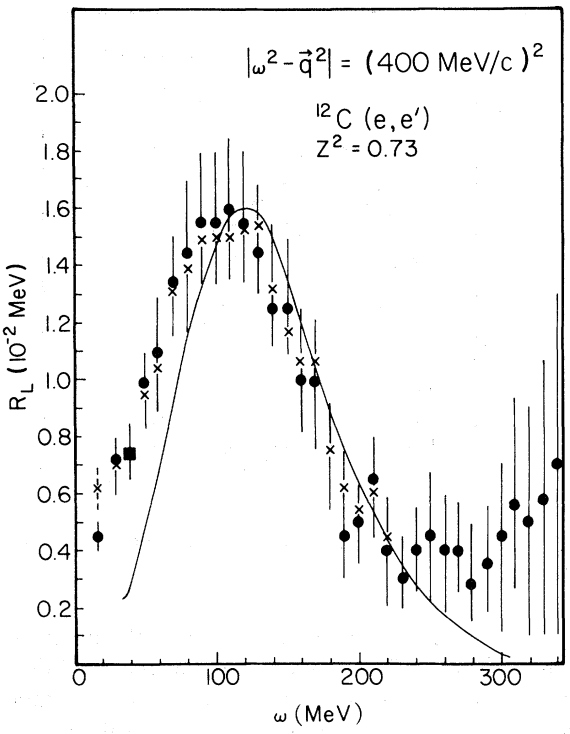

FIG. 14. The longitudinal response function, $R_L(\vec{q},\omega)\equiv 4\pi S_L(\vec{q},\omega)/M_T$ for inelastic electron scattering from ^{12}C. (Here M_T is the mass of the target.) The solid line shows the modified impulse approximation with $Z^2=0.73$. The data are from Ref. 2. Note that $q_\mu{}^2=|\omega^2-\vec{q}^{\,2}|=(400\ \mathrm{MeV}/c)^2$.

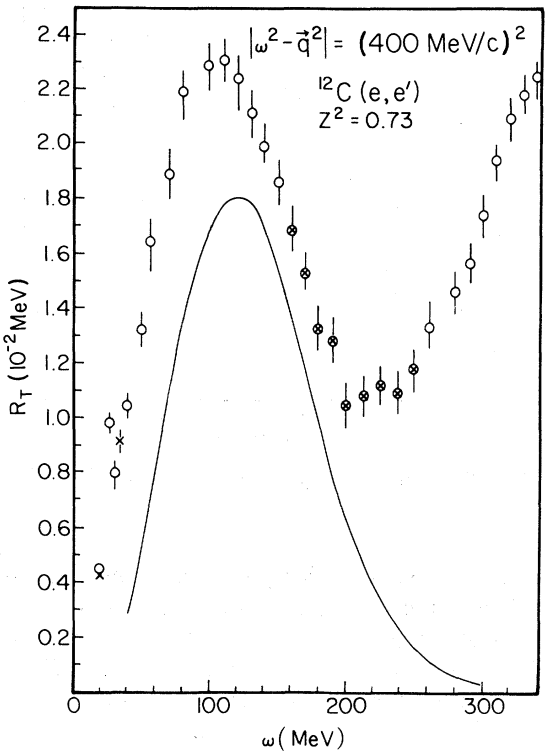

FIG. 15. The transverse response function, $R_T(\vec{q},\omega)\equiv 4\pi S_T(\vec{q},\omega)/M_T$ for inelastic electron scattering from ^{12}C. The solid line shows the modified impulse approximation with $Z^2=0.73$. The data are from Ref. 2.

strength for small values of ω below the quasi-elastic peak. If we assume that this strength has been shifted out of the peak region by collective effects we can argue that the data for S_L for ^{56}Fe can also be understood if we put $Z^2=0.7$ and ascribe the enhanced discrepancy at the peak to the aforementioned collective effects arising from particle-hole rescattering. With this alternative value of Z^2 we have $Z\sim 0.84$, which is about the upper limit for the orbital occupation probability obtained in the calculations summarized in Ref. 7. An analysis of the longitudinal response which does not completely neglect collective effects is called for. However, we believe that the uncertainty in Z which we suggest for this effect represents a reasonable estimate that will be supported by further investigation.

Finally, we consider the comparison between theory and experiment for quasi-elastic scattering from ^{12}C. This nucleus is less dense than ^{56}Fe and nuclear matter results are less useful here. In Fig. 14 we present a comparison of the data with the modified impulse approximation. Here $Z^2=0.73$, and the fact that this value ($Z=0.85$) is larger than the value for ^{56}Fe ($Z=0.77$) is consistent with the density dependence expected for the mean occupation factors.[7] In Fig. 15 we compare the modified impulse approximation for the transverse response function, $R_T(\vec{q},\omega)$, with the experimental data.[2] Here an enhancement of the unmodified response of about 40 percent is required, if upon further multiplication by $Z^2=0.73$, one is to obtain agreement with the data. Again, there is some degree of uncertainty in the value given for Z due to the presence of some small collective effects in the longitudinal response. (See Fig. 14.)

V. CONCLUSIONS

We have adopted the point of view that we can understand the longitudinal response function if we assume that a significant amount of the longitudinal strength is to be found at high energies, and that the depletion of strength at the lower energies is a measure of the reduction of the shell-model orbital

occupation probability, P, from unity due to short-range correlations. The probability of occupation of a shell model orbital in Fe appears to be slightly less than 0.8. This value is consistent with the theoretical values for this factor obtained in Brueckner-Hartree-Fock calculations. For ^{12}C one infers $P \simeq 0.85$. This larger value can be understood if one notes the smaller density of the ^{12}C system relative to Fe.

This interpretation of the experimental data leads to a more marked disagreement between the calculated and experimentally determined transverse response function, indicating even larger meson current effects than might have been considered to be present on the basis of a comparison of the experimental data with the *unmodified* impulse approximation. It is clear that there is much work to be done in order to obtain an accurate quantitative description of the transverse response.

ACKNOWLEDGMENTS

This work was supported in part by a grant from the National Science Foundation and the PSC-BHE Award Program of the City University of New York.

---

*On leave from the University of Calabar, Calabar, Nigeria.

[1]R. Altemus, A. Cafolla, D. Day, J. S. McCarthy, R. R. Whitney, and J. E. Wise, Phys. Rev. Lett. 44, 965 (1980).

[2]P. Barreau *et al.*, Nucl. Phys A358, 287 (1981).

[3]J. V. Noble, Phys. Rev. Lett. 46, 412 (1981).

[4]T. W. Donnelly, J. W. van Orden, T. de Forest Jr., and W. C. Hermans, Phys. Lett. 76B, 393 (1978), and references therein.

[5]M. Kohno and N. Ohtsuka, Phys. Lett. 98B, 335 (1981).

[6]Y. Horikawa, F. Lenz, and C. Mukhopadhyay, Phys. Rev. C 22, 1680 (1980).

[7]M. A. Preston and R. K. Bhaduri, *Structure of the Nucleus* (Addison-Wesley, Reading, Mass., 1975), see Chap. 8 and Table 8.8.

[8]A. L. Fetter and J. D. Walecka, *Quantum Theory of Many-Particle Systems* (McGraw-Hill, New York, 1971), see Chap. 5, Sec. 17.